INCREASED SALINITY DECREASES ANNUAL GROSS PRIMARY PRODUCTIVITY OF A NORTHERN CALIFORNIA BRACKISH WETLAND

by

Sarah Russell

A THESIS SUBMITTED IN PARTIAL FULFILLMENT OF

THE REQUIREMENTS FOR THE DEGREE OF

MASTER OF SCIENCE

in

THE FACULTY OF GRADUATE AND POSTDOCTORAL STUDIES

(Geography)

THE UNIVERSITY OF BRITISH COLUMBIA

(Vancouver)

December 2021

The following individuals certify that they have read, and recommend to the Faculty of Graduate and Postdoctoral Studies for acceptance, a thesis entitled:

Increased salinity decreases annual gross primary productivity of a Northern California brackish wetland

submitted by Sarah Russell in partial fulfillment of the requirements for the degree of Master of Science in Geography

Examining Committee:

Dr. Sara Knox, Geography, UBC
Supervisor

Dr. P. Oikawa, Earth & Environmental Sciences, Cal State East Bay
Supervisory Committee Member

Dr. Mark Johnson, Institute for Resources, Environment and Sustainability, UBC
Supervisory Committee Member

Dr. Ian McKendry, Geography, UBC
Additional Examiner

Abstract

Brackish wetland plant and microbial communities are a diverse mix of freshwater- and saltwater-adapted species in competition with each other. This has led researchers to predict that carbon cycling in brackish wetlands may be more resilient to changes in salinity than in fresh- or saltwater systems. Rush Ranch, a brackish tidal wetland near Suisun Bay, California, experienced drought-induced salinization in the 2015 and 2016 growing seasons followed by a freshwater flushing event in 2017. During the drought, salinity rose from the baseline of 4.5 ppt to an average of 10.3 ppt, peaking at 12.5 ppt. During these summers, gross primary productivity (GPP) decreased by 30%. Stepwise linear regression revealed that salinity was a major driver of GPP at this brackish wetland. We trained a random forest model to predict GPP based on environmental data from low salinity years. Naive to the salinization event, the model over-predicted GPP during high salinity years. These results provide ecosystem-scale evidence that increased salinity can decrease GPP at brackish tidal wetlands. This relationship is a starting point for incorporating the effect of changes in salinity on GPP in wetland carbon models, which could improve wetland carbon forecasting and management for climate resilience.

Lay Summary

Wetlands are important ecosystems because they take carbon dioxide out of the atmosphere and store it for a long time. Coastal wetlands experience different levels of saltwater. Brackish wetlands are less saline than the ocean, but more saline than freshwater wetlands. Rush Ranch, a brackish tidal wetland near Suisun Bay, California, experienced abnormally high levels of salinity from 2014 to 2015 as the result of a statewide drought. During these summers, gross plant productivity (GPP) decreased by 30%, representing a loss of stored carbon. Stepwise linear regression revealed that salinity was a major driver of GPP at this brackish wetland. These results provide ecosystem-scale evidence that increased salinity can decrease GPP at brackish tidal wetlands. This relationship is a starting point for incorporating the effect of changes in salinity on GPP in wetland carbon models, which would help wetland managers predict how much carbon a given wetland will store.

Preface

I was responsible for analyzing flux data obtained from Ameriflux site US-Srr, otherwise known as Rush Ranch, a brackish wetland in Northern California. This high-frequency flux data was processed and gap-filled by my supervisor, Dr. Sara Knox, Dr. Ellen Stuart-Haetjens. I used the R package, REddyProc (V2.2.0) by Thomas Wutzler.

Table of Contents

List of Tables

List of Figures

List of Abbreviations

Abbreviation	Definition
AIC	Akaike information criterion
ANN	Artificial neural network
C	Carbon
CH_4	Methane
CO_2	Carbon dioxide
DIC	Dissolved inorganic carbon
DOC	Dissolved organic carbon
ER	Ecosystem respiration
GHG	Greenhouse gas
GPP	Gross primary productivity
NDVI	Normalized difference vegetation index
NEE	Net ecosystem exchange of CO_2
LAI	Leaf area index
PAR	Photosynthetically active radiation
ROL	Radial oxygen loss
TA	Air temperature
TEA	Terminal electron acceptors
TS	Soil temperature
VPD	Vapor pressure deficit
WTD	Water table depth

Acknowledgements

Thank you to Dr. Sara Knox, for being the most brilliant and supportive supervisor imaginable. Also thank you to Dr. Patty Oikawa, Dr. Lisa Windham-Meyers, and Dr. Ellen Stuart-Haentjens for providing insight and expertise every step of the way. Thank you to the additional members of my committee, Dr. Mark Johnson and Dr. Ian McKendry.

Dedication

This thesis is dedicated to my family, for continually supporting me during my decades of education, as well as my husband and Bella, who have brightened the last three years considerably.

Chapter 1: Introduction

Increased anthropogenic emissions of greenhouse gases from burning fossil fuels in the last hundred years are causing the earth's atmosphere to warm. Unless we achieve net zero carbon emissions before 2030, the atmosphere will continue to warm by a total of at least 1.5°C.[1,2] This will dramatically change the weather, hydrology, biotic communities, and carbon cycling of all ecosystems. Ecosystems tend to emit more carbon dioxide post-disturbance,[3] representing an additional anthropogenic source of carbon emissions and a potential positive climate feedback loop. For example, accelerated sea level rise may displace carbon-sequestering wetlands,[4,5] reducing the global carbon sink.

In an effort to incentivize corporations to decrease their greenhouse gas emissions, economists have suggested taxing commercial carbon emissions. Beyond carbon pricing, some governments allow companies to trade for the right to emit carbon beyond an emissions "cap" using a credit system (cap-and-trade). Funds used to purchase carbon credits are then used to offset the additional emissions. Cap-and-trade has been adopted in the European Union, Quebec, California, South Korea, and New Zealand. In California carbon offsets include planting trees, offsetting ozone emissions, or capturing methane from mines, livestock manure, or rice paddies.

Conservationists and ecologists have promoted the inclusion of wetland restoration in carbon markets for the last decade.[6,7] Though wetlands make up a much smaller portion of the earth's land cover, with a global average carbon burial rate of 8.0 ± 8.5 tons of CO_2 equivalent ha^{-1} y^{-1},[8] wetlands sequester almost as much carbon as all terrestrial forests combined,[9] making them attractive candidates for carbon offset restoration projects. Due to constant exposure of peat to oxygen, drained wetlands experience higher rates of peat decomposition and release more

carbon dioxide than wetlands with hydrologic connectivity.[10] Agriculture in drained wetlands is often unsustainable due to subsidence (loss of peat elevation), which increases the likelihood of inland saltwater intrusion. Land subsidence is especially concerning in areas where people rely on groundwater for drinking water, such as the Sacramento-San Joaquin River Delta in California and the Rijnland water board in The Netherlands[11,12] Cap-and-trade funds could be used to restore these freshwater wetlands and to support residents as they transition from farming to other industries.

Despite the ability of coastal wetlands to sequester large amounts of carbon, restoration projects have not entered most carbon markets. Tidal saltwater wetlands have been shown to store as much carbon as freshwater wetlands while emitting much less methane.[13] An estimated 67% of the world's salt marshes have been starved of sediment or drained for agriculture and development,[8] turning them into anthropogenic carbon sources. Though at least four restoration methodologies have been developed, wetland restoration has been slow to enter carbon markets. To date, only one wetland restoration project has been registered as a carbon offset in the United States.[7] This may be because the published restoration methodologies tend to be site-specific and complicated to implement.

A simple forecasting methodology is needed to allow coastal wetland restoration to enter carbon markets as an emissions offset. The majority of wetlands are inland freshwater, so less research has been done to create simple, process-based models that can be used to forecast carbon dynamics across coastal wetland sites. In this literature review, I will describe wetland carbon cycling, its environmental drivers, and previous wetland carbon modeling work. Finally, I will outline what is necessary to develop a simple, process-based model that forecasts coastal wetland carbon dynamics.

1.1 The Wetland Carbon Cycle

Carbon takes many forms in wetlands. It is transiently stored in vegetation and the rhizosphere during the growing season. During the growing season, carbon is released from roots in the form of root exudates. When wetland vegetation senesces in the autumn, leaf and root biomass is released into the top layers of soil. Soil inundation creates anoxic conditions that prevent biomass decomposition and promote peat accretion. This is where carbon is stored over long timescales (Figure 1).

Net ecosystem exchange (NEE) is the net flux of carbon dioxide between ecosystems and the atmosphere. The amount of carbon dioxide wetlands sequester is largely determined by the balance between gross primary productivity (GPP) and ecosystem respiration (ER) during the growing season. The bulk of carbon dioxide emissions take the form of ER. The ratio of GPP to ER is dependent on the environmental conditions and varies by site (Section 3.1). A portion of GPP enters the soil as root exudates that can be converted into methane by methanogenic microbes along with a fraction of bulk peat under anoxic conditions.[14] Methanogenesis is also heavily dependent on environmental factors (Section 3.2).

NEE can be determined using either point or ecosystem-scale measurements. Chamber-based (point) methods have been used longer and comprise the majority of measurements of wetland carbon flux. Chamber-based measurements have the advantage of having a precise footprint but the disadvantage of small spatial and temporal scale. In carbon inventories, point chamber measurements must be scaled up to represent whole ecosystems across the entire year, introducing uncertainty to NEE estimates. Also, researchers can bias chamber-based methane measurements during chamber set-up by increasing pressure on the soil, increasing methane ebullition.[15]

Eddy covariance is an ecosystem-scale method of measuring NEE. It has greater spatial and temporal scales than chamber-based measurements. By observing the amount of carbon dioxide or methane that flows up and down in eddies of air and averaging these high-frequency measurements over half an hour, one can estimate the total amount of carbon emitted or absorbed by a large expanse of the ecosystem.[16] One disadvantage of eddy covariance is its high cost and maintenance. It is also notoriously difficult to close the energy balance of ecosystems using eddy flux observations for several reasons, including the fact that point radiation measurements taken at the tower location might not represent the entirety of the eddy flux footprint.

Since there is no direct way to measure whole-ecosystem GPP and ER individually, NEE must be partitioned in order to obtain estimates of photosynthesis and respiration. The two dominant flux partitioning methods are daytime- and nighttime-based. Flux partitioning based on daytime values fits the Light Response Curve of NEE to radiation.[17] Nighttime-based flux partitioning fits nighttime NEE (assumed to be entirely ER) to temperature and uses that to model ER in the daytime.[18] These simple methods are used widely but may not apply to ecosystems where ER and GPP are dependent on environmental variables beside temperature or radiation.[19] For example, water table depth is a strong driver of wetland ER, since decomposition is suppressed by the anoxic conditions of high tide. A standardized method of partitioning wetland NEE that accounts for these factors should be developed.

Throughout the year, dissolved organic and inorganic (DOC and DIC respectively) carbon enters minerotrophic wetlands from hydrologic inputs. This can cause mineral carbon to build up in alluvial deposits adjacent to fast-flowing water. Carbon also exits wetlands through tides, groundwater, runoff, or channelized flow. Together, these hydrologic carbon inputs and outputs are referred to as lateral carbon flux. Lateral flux has been proven to represent a sink

proportional to carbon burial in mangrove ecosystems, since DIC exported to the oceans is either released as carbon dioxide or is sequestered as DIC for long residence times (~100,000 years).[20] Few measurements of lateral carbon flux have been made in wetlands, where hydrological inputs and outputs can be difficult to locate and observe. This knowledge gap must be filled in order to accurately model carbon sequestration in wetlands, especially in coastal wetlands where tides pose a significant potential route for lateral carbon flux.

1.2. Biophysical Drivers of Wetland Carbon Dynamics

1.2.1 Net Ecosystem Exchange

Gross primary productivity and ecosystem respiration are influenced by many of the same environmental factors. The type and amount of vegetation determines the maximum rate of photosynthesis and therefore GPP per unit area. Several greenness indices can be used to quantify vegetation amount, including leaf area index (LAI), Normalized Difference Vegetation Index (NDVI), and solar-induced chlorophyll fluorescence (SIF), which can be remotely sensed or determined from field-based images. Different plant species are more productive than others. Growing season length also determines net annual GPP, with wetlands at higher latitudes experiencing shorter growing seasons and therefore less net annual GPP.[3] Ecosystem respiration is also directly affected by GPP since the majority of labile carbon available to decomposers is released from plants within the same growing season and bulk peat is composed mainly of plants from previous growing seasons.[21]

Ecosystem photosynthesis and respiration have similar responses to air temperature. Photosynthetic rate is highest at an optimal temperature that varies by wetland type and latitude. This value can either be measured by taking leaf cuvette- or chamber-based measurements of photosynthesis at a range of temperatures or by partitioning eddy-flux NEE measurements and fitting GPP to air temperature.[22] Ecosystem respiration increases with temperature according to the Arrhenius function. Respiration also has an optimal temperature, related to the heat capacity of microbial enzymes, but this optimum tends to be higher than the optimum for photosynthesis.[23]

Increasing soil moisture or water table depth create anoxic conditions that lower the rate of soil respiration. The reliable suppression of ER during high tide is one of the reasons coastal

wetlands are efficient carbon sinks. Bypassing the water column, oxygen can travel down vegetation aerenchyma into inundated soil in the rhizosphere in a process called radial oxygen loss (ROL), creating oxygenated pockets where soil respiration can occur at higher rates.[24,14] Carbon dioxide can then be released from these pockets via plant-mediated transport, ebullition, or diffusion through the water table. Unusually high tides that submerge plants suppress GPP,[25] which is concerning in light of projections of sea level rise (Section 3.3).

Lateral carbon transport can either increase ER by providing more organic matter for decomposition or decrease it by transporting organic matter out of the system. This transport can also increase or reduce ER by changing the soil type and amount of alternate electron acceptors dissolved in the water column.

Global climatological events can affect wetland NEE. Though coastal wetlands are not typically water-stressed during regional droughts, salinity and sulphate content can accumulate in wetlands as upland runoff decreases. High levels of salinity and sulphate can stress wetland plants and suppress GPP, creating interannual variability in cumulative carbon uptake in wetlands.[26,27] The relationship between salinity and GPP varies by site. Wetland vegetation closer to the coast is adapted to high salinity and is just as productive as brackish wetlands under low salinity.

1.2.2 Methane Exchange

Wetland methane exchange and NEE share many biophysical drivers. This could be convenient from a modelling perspective, because it can reduce the number of variables needed to adequately reproduce observed carbon dynamics. On the other hand, many environmental conditions promote both carbon dioxide sequestration and methanogenesis, making it difficult to

predict the net climate forcing produced by wetland restoration unless both processes can be accurately forecasted.

All the factors that impact GPP indirectly impact methanogenesis, since the bulk of carbon substrates used by methanogens is released into the labile carbon pool within the growing season as root exudates.[14] Longer growing season length increases cumulative methane emissions. Inundated wetlands that have more vegetation cover will produce more methane.[28] Increasing temperature will also increase methanogenesis, as substrates will be more likely to intercept extracellular methanogenic enzymes. But increasing temperature also increases methane oxidation, attenuating the temperature response.

Methane exchange is heightened in the anoxic conditions created during wetland inundation because methanotrophs use oxygen to oxidize methane into carbon dioxide, making water table depth and soil moisture two of the strongest drivers of methanogenesis in wetlands. Methane must travel through the soil and water column without being oxidized in order to be released to the atmosphere. Dissolved methane that diffuses through the water table, allowing it to encounter oxidative species via Michaelis-Menten kinetics. But there are alternative routes methane can take to bypass oxidation (Figure 1). When atmospheric pressure increases, dissolved methane can form bubbles and rise to the surface in a process called ebullition.[29]

Plant-mediated transport can also allow methane to bypass oxidation. Methane can enter roots and travel up through plant aerynchyma, bypassing the one of oxidation.[29,28] This explains why certain vegetation types (such as rice and marsh grasses) release more methane than others. The condition of the vegetation also impacts plant-mediated transport of methane. Aerenchymatous plants that are snapped or have begun to senesce can allow more methane to exit the plant and enter the atmosphere.[28] Wind conditions also impact how much methane can

be transported through plants. Negative air pressure created by wind will be more likely to draw methane up the plant, rather than transport oxygen down into the soil where it can be used by methanotrophs.[28]

Methanogens are the least competitive heterotrophic microorganisms in wetland soils. In anoxic conditions, they are outcompeted by sulfate-reducing bacteria when sulphate is available and other microbes when terminal electron acceptors (TEAs) such as Fe (III), Mn (II, III), or NO_3^- are present.[14] Rhizosphere ROL can re-oxidize TEAs, further limiting methane exchange in inundated wetlands.[14] Salinity and sulphate content are closely correlated, so less methanogenesis occurs in saline coastal wetlands than in freshwater wetlands.[13] Since salinity is easier and more cost-effective to measure it can be used as a proxy for sulphate concentration.[13]

1.2.3 Sea-Level Rise

Coastal wetlands have historically gained elevation fast enough to keep pace with sea-level, but predictions of rates of sea-level rise in 2100 are an order of magnitude higher than current rates.[4] Additionally, sea-level rise will not be uniform around the globe. Northern North America will experience less sea-level rise than the southern Northern America.[4] Coastal wetlands that have high rates of peat accumulation, plenty of undeveloped upland to migrate to, and lower projected rates of sea-level rise have the best chance of surviving the Anthropocene.[5] Wetland loss due to sea level rise is a greater concern where degradation has led to subsidence or decreased rates of peat accumulation.

Though we can predict peat accumulation across plant community types, there is little data on the effect of increased flooding on wetland vegetation. It is assumed that low, middle, and high marsh plant species will be able to migrate inland at the pace of sea-level rise, but if this

is not the case sea-level rise could pose a greater threat to coastal wetland productivity and therefore peat accumulation. Conversely, wetland management (such as levee systems) could prevent loss of wetlands due to sea-level rise.

1.3. Wetland Carbon Models

Wetland carbon models exist at a range of complexities based on many factors, including the length of their time step (annual, daily, or sub-daily), their spatial range, whether they are empirical or mechanistic. Furthermore, mechanistic models can vary widely in how many processes and carbon pools they simulate. Empirical carbon models typically fit observations of carbon flux to environmental variables like temperature and soil moisture. Mechanistic models use prior knowledge about ecosystem processes to estimate carbon fluxes based on environmental variables. Both model types can be parameterized for one or more sites.

Wetland accretion models simulate long-term changes in wetland height. They can also be used to obtain crude estimates of annual carbon emissions. These models are typically parameterized using peat core and paleoclimate data with few carbon pools and an annual time step. Since peat accumulates so slowly models must be run for hundreds of years in order to forecast trends. Peatland accretion models include the Peatland Decomposition Model, the Marsh Equilibrium Model, and the Wetland Accretion Rate Model of Ecosystem Resilience (PDM, MEM, and WARMER respectively; Table 1). The first peat accretion models focused on simulating freshwater peatland formation. To predict coastal wetland peat accumulation in the Anthropocene accretion models had to be modified to account for sea-level rise.[30,31]

Short-term wetland carbon models are used to simulate fluxes throughout the year and typically provide only a crude estimate of peatland accumulation. Inclusion of more carbon pools allows short-term models to simulate interannual variability caused by the biophysical drivers discussed in Section 3. Biomass can be split into above- and below-ground or broken down by plant functional type. Soil carbon can be separated into labile and recalcitrant pools or broken down by size to explicitly model the chemical reactions of methanogenesis and methanotrophy.[14]

Increased complexity can make models more difficult to parameterize, because of the amount of data required and the effects of equifinality.

One model of methane production in coastal wetlands ($CH4MOD_{wetland}$) has been developed, but it does not simulate GPP or ER.[32] Furthermore, it requires soil texture, soil redox potential, soil organic matter, and soil bulk density as inputs—data that is not always readily available for wetland sites managed by municipalities and conservationists. A simpler, more flexible model is needed to predict the complete carbon dynamics of coastal wetlands.

The Peatland Ecosystem Photosynthesis, Respiration, and Methane Transport model combined with the Dual Arrhenius Michaelis-Menten model (PEPRMT-DAMM) represents a middle ground between complexity and flexibility. The core modules of PEPRMT only require six environmental variables to run (GPP, photosynthetically active radiation, water table depth, a greenness index, and air temperature) and can be parameterized for different sites.[33] The addition of the DAMM model allows for a more process-based simulation of extra-cellular enzymatic reactions that occur during decomposition, methanogenesis, and oxidation. PEPRMT was parameterized using data from freshwater, non-tidal wetlands in California, but is modular enough to be easily modified, re-parameterized, and even incorporated into other models. Its simplicity keeps its run-time short, making it ideal for the development of an online tool for policymakers to perform their own analyses.

A simple model like PEPRMT could be developed into an accessible means of forecasting the carbon emissions of coastal wetlands post-restoration. Since most emissions models were developed for freshwater wetlands, a modified version of one will be needed to simulate coastal wetland carbon emissions. It would need to include 1) lateral transport of carbon and 2) the effects of salinity on GPP, ER, and methane exchange.

To make this model predictive, it would need a module that forecasts GPP and projections of its other input values. Projections of water table depth and salinity require site-specific knowledge of climate and hydrology. Long-term predictions of carbon emissions will require linking this model to a long-term peatland accretion model that can predict wetland elevation and productivity as sea levels rise. The effects of restoration on coastal wetlands should also be accounted for. Once a model that forecasts the carbon sequestration potential of restored coastal wetlands has been developed, the results will need to be presented in a form that stakeholders can use to translate into carbon offsets and management decisions.

1.4 Summary

In order to meet ambitious emissions reduction targets, many countries plan to restore or manage landscapes for carbon sequestration.[1,35,36] Coastal wetland restoration is an excellent candidate for such projects, since they are among the most productive ecosystems, providing long-term storage of 151 g C m^{-2} yr^{-1} on average[37,38] Meanwhile 25% of coastal wetland area has been degraded globally since 1800 due to land development and species invasion.[39,9,40] Degraded coastal wetlands have become carbon sources, emitting 0.2-2.4 Pg CO_2 yr^{-1} globally,[41] providing an even greater incentive for restoration and conservation. More precise predictions of wetland carbon sequestration not only aid in tidal wetland preservation and restoration efforts, but also make it easier to implement wetland restoration as an offset in carbon markets—an area where wetland restoration projects have struggled to gain widespread traction.[7]

Brackish wetland carbon dynamics are especially tricky to characterize because of their unique geography. They exist at the cusp between freshwater and saltwater, experiencing various amounts of tidal action and upland freshwater input, such that individual brackish wetlands can accumulate carbon at different rates[42]. Brackish wetland plant and microbial communities are a diverse mix of freshwater- and saltwater-adapted species in competition with each other.[43,44,14] This has led researchers to predict that carbon cycling in brackish wetlands may be more resilient to changes in salinity than in fresh- or saltwater systems.[45] This assumption should be tested, as brackish wetlands are expected to experience more frequent and extreme variations in salinity due to drought, excessive precipitation, storm surges, and sea-level rise.[46] We must know how these disturbances will impact brackish wetlands in order to manage them for climate resilience and forecast their potential carbon sequestration under climate change.

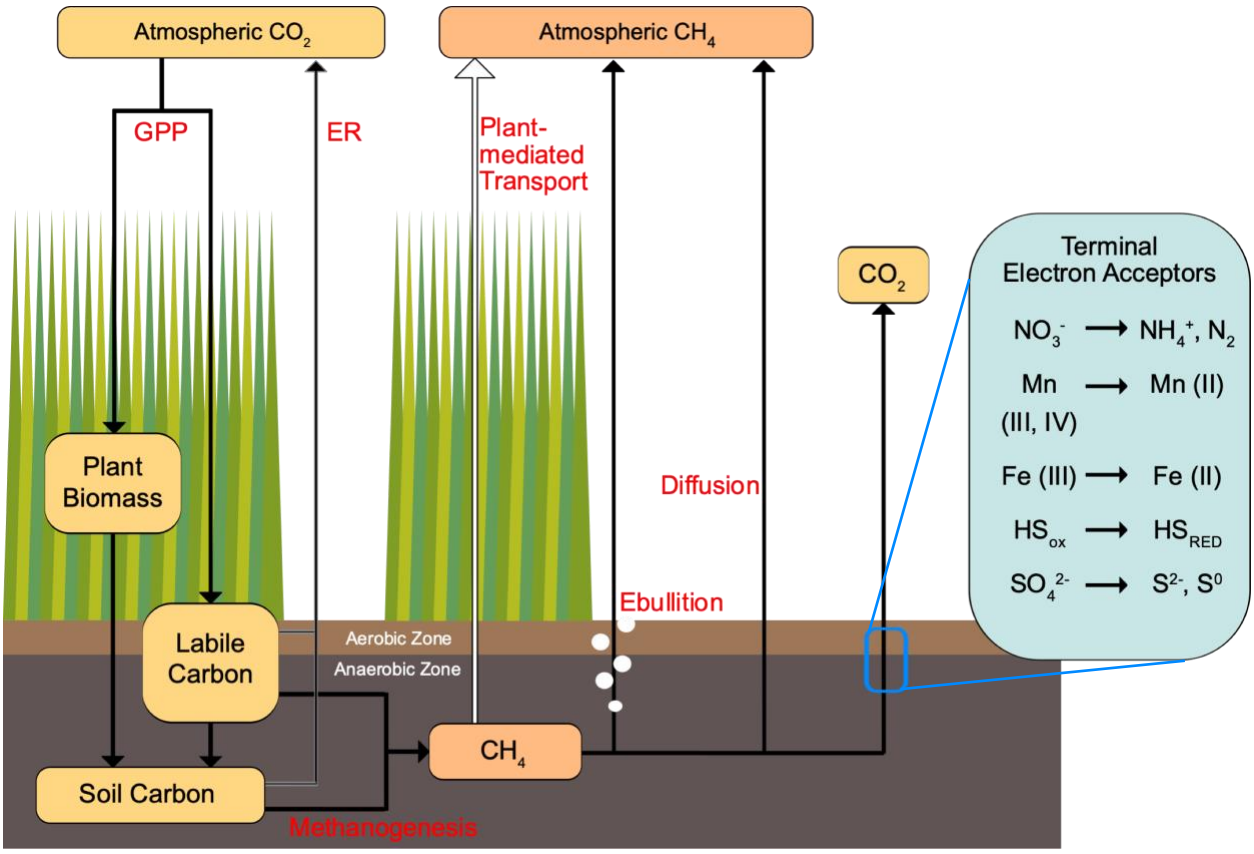

Figure 1. Carbon cycle of coastal wetlands. Carbon pools shown in boxes, methane shown in orange. Processes shown in red. GPP = gross primary production. ER = ecosystem respiration. Adapted from Oikawa et al., 2017a and Bridgham, 2013.

Model	Outputs	Inputs	Time Step	Spatial Range	Reference
Peat Accumulation					
MEM	MSL, Accretion, Biomass	SLR, SSC, initial elevation, above-/belowground biomass, RTS, MSL, MHW	Annual	Site	Byrd et al., 2016
Hydro-MEM	MLW, MHW, Accretion, Elevation, Biomass productivity	MEM inputs + Astronomic tides, Bottom friction	5/10/50 years	Spatially explicit	Alizad et al., 2016
WARMER	Accretion, Elevation	Cohort-based veg, SLR, Organic matter, Porosity, Sediment	Annual	Site	Swanson et al., 2014
PDM	Mass and decomposability for each peat layer	Above -and below-ground NPP, WTD, Rooting depth, Peatland age	Annual	Site	Frolking et al., 2001
Mechanistic Emissions					
PEPRMT-DAMM	Freshwater CO_2, CH_4	GPP, PAR, WTD, LAI/NDVI, Temp	Sub-daily	Site	Oikawa et al., 2017a
$CH4MOD_{wetland}$	Coastal CH_4	Soil texture, Temp, Soil redox potential, WTD, Soil sand fraction, SOM, Annual NPP, Bulk density	Daily	Site	Li et al., 2016
Wetland-DNDC	Freshwater CO_2, CH_4	Biomass, SOC, pH, Porosity, Surface inflow/outflow, Respiration rate, Max/min/optimal GDD, Temp, Precip, Solar radiation	Daily	Site	Zhang et al., 2002
Empirical Emissions					
PEPRMT	Freshwater CO_2, CH_4	GPP, PAR, WTD, LAI/NDVI, Temp	Sub-daily	Site	Oikawa et al., 2017a

Table 1. An incomplete summary of wetland carbon models. Models: MEM = Marsh Equilibrium Model; WARMER = Wetland Accretion Rate Model of Ecosystem Resilience; PDM = Peatland Decomposition Model; PEPRMT = Peatland Ecosystem Photosynthesis, Respiration, and Methane Transport; DAMM = Dual Arrhenius Michaelis-Menten; $CH4MOD_{wetland}$ = Wetland Methane Model; Wetland-DNDC = Wetland DeNitrification DeCompostion; Variables: GDD = growing degree days, GPP = Gross Primary Productivity, LAI = Leaf area index, MHW = mean high water, MLW = mean low water, MSL = mean sea level, NDVI = normalized difference vegetation index, NPP = net primary productivity, PAR = photosynthetically active radiation, RTS = root-to-shoot ratio, SLR = sea-level rise, SOC = soil

organic carbon, SOM = soil organic carbon, SSC = suspended sediment concentration, WTD = water table depth.

Understanding the environmental drivers of coastal wetland carbon dynamics is key to predicting and optimizing carbon sequestration. Sudden sustained increases in porewater salinity caused by regional drought (i.e., drought-induced salinization)[27,47] and flood-induced desalinization events[45,48] have been shown to impact net ecosystem exchange of CO_2 (NEE) at freshwater and saltwater tidal wetlands, respectively, but it is unclear if such events influence NEE at brackish tidal sites, where plant and microbe communities are adapted to smaller daily fluctuations in salinity.[42] Determining the causes of interannual variability in carbon sequestration at brackish tidal wetlands could inform decisions about wetland restoration for carbon storage.In order to better forecast seasonal and interannual variability in carbon dynamics of brackish marshes, we need a better understanding of the drivers of that variability. To this end, our study sought the cause of high variability in annual NEE at a brackish wetland in Northern California during a period that coincided with drought-induced salinization.

Chapter 2: Methods

Data was collected at Rush Ranch from March 2014 through September 2018. Rush Ranch is an intact brackish tidal wetland located in Suisun Bay, California in the San Joaquin River Delta. It has a mean tidal range of 1.72 m.[49] Rush Ranch experiences a Mediterranean climate, with hot, dry summers and cool, wet winters. Plant species include *Schoenoplectus* sp., *Typha* sp., *Juncus balticus*, *Distichlis spicata*, *Sarcocornia pacifica*, and *Lepidium latifolium*.[49] Rush Ranch experienced drought-induced salinization in the 2014, 2015, and 2016 growing seasons followed by a flushing event in January-February 2017. During drought growing seasons, salinity rose from the baseline annual average of 4.5 ppt (based on 2017-2018) to an average of 10.3 ppt. In August of 2015, salinity peaked at 12.5 ppt (Fig. 2). These salinities are well within the range of brackish wetlands (0.5-18 ppt) but represent a drastic increase from baseline conditions at Rush Ranch.

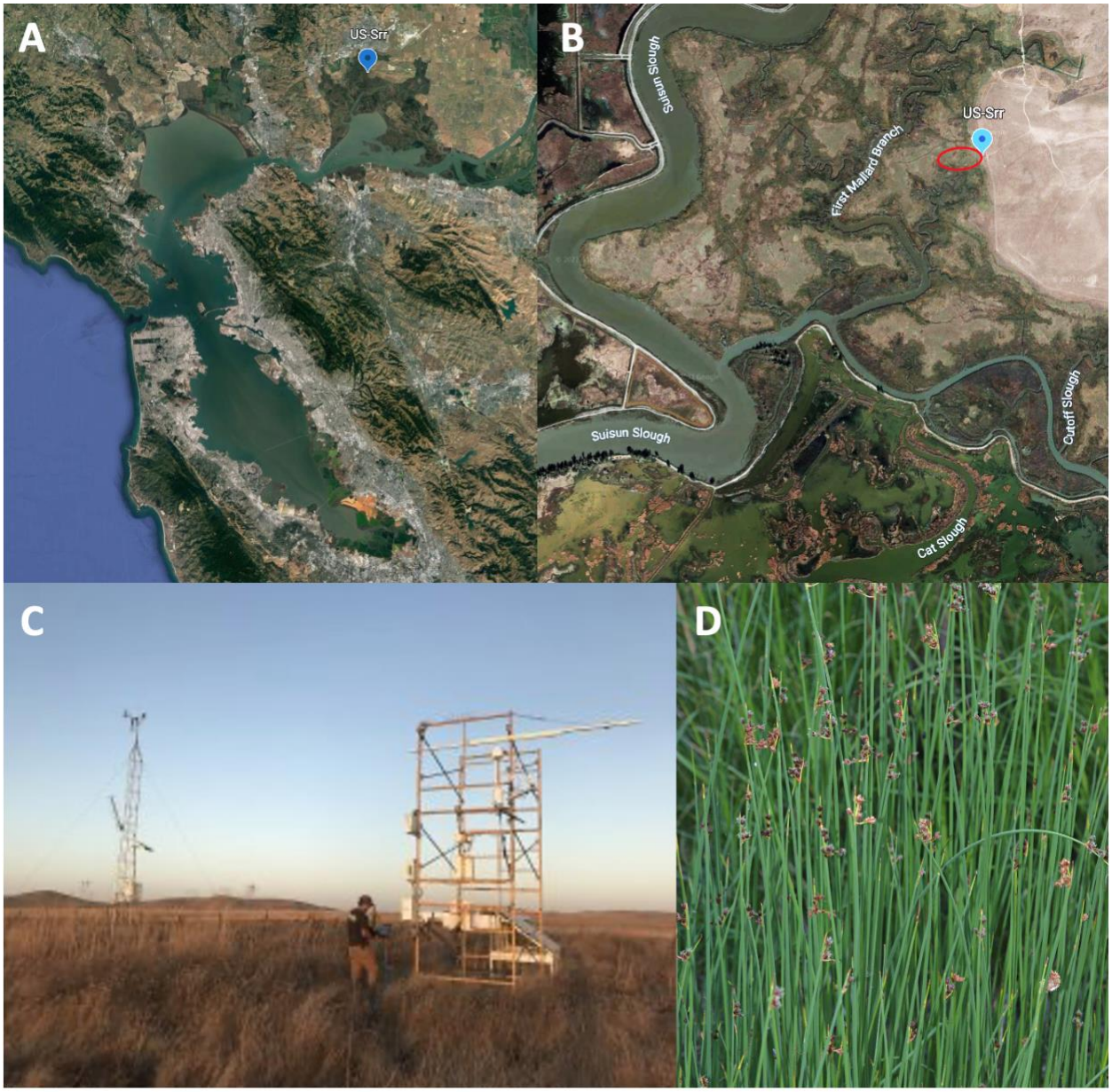

Figure. 2 Ameriflux US-Srr Study Site in Rush Ranch. A) Rush Ranch is located in the San Joaquin River Valley of California near Suisun Bay. **B)** An approximation of the growing season daytime flux tower footprint is pictured in red.[50] **C)** US-Srr measures an area of high marsh with infrequent flooding. Photo taken by Ellen Stuart-Haetjens. **D)** Vegetation at the site is dominated by bulrushes (pictured here) and increasingly influenced by pepperweed (*Lepidium latifolium*).

The eddy covariance method was used to measure land-atmosphere exchanges of CO_2 (NEE; μmol m^{-2} s^{-1}), water vapor (W m^{-2}), and sensible heat (W m^{-2}) at Rush Ranch (Ameriflux site US-Srr). An open-path infrared gas analyzer (LI-7500, LI-COR Biogeosciences, Lincoln, NE, USA) was used to measure fluctuations in CO2 and H2O molar density, and high frequency 3D wind speed components and virtual temperature were measured with a sonic anemometer (CSAT3, Campbell Scientific, Logan, UT, USA) mounted 3.4 m above the soil. Auxiliary environmental measures included vapor pressure deficit (VPD; kPa), precipitation (mm), PAR, and air temperature (ºC). Salinity and channel depth data was obtained from the NOAA station (ID 9415096) in Suisun Bay.

We gap-filled NEE using the median of 50 iterations of an ANN model trained on meteorological variables. More details can be found in Knox et al., 2015.[51] We then calculated ecosystem respiration (ER) as the median of 50 iterations of an ANN trained on nighttime NEE.[50] Gross primary productivity (GPP) was calculated as the difference between NEE and ER. NEE was also partitioned using daytime and nighttime methods using the REddyProcWeb online tool for comparison.[18,52] We then calculated the yearly cumulative sums of these fluxes, using April 1st (the first growing season day) as the beginning of the year.

Since random error in flux estimates has been shown to be negligible at this site, uncertainty was approximated as gap-filling error. Cumulative uncertainties of NEE and ER were calculated as the standard deviation of each set of 50 ANN-generated timeseries. For half-hours where observed NEE values were available, cumulative uncertainty of GPP was calculated as $sd(NEE_{obs} - ER_{ANN})$, where ER_{ANN} represents the 50 iterations of ER produced by the ANN model. For gap-filled half-hours, cumulative uncertainty of GPP was calculated as the standard

deviation of the 2,500 combinations of $NEE_{ANN} - ER_{ANN}$, where NEE_{ANN} represents the 50 iterations of NEE produced by the gap-filling ANN.

We used simple linear regression to compare annual growing season GPP to environmental variables related to drought (salinity, air temperature, VPD, and precipitation) measured at the site. A correlation plot, made using the 'corrplot' package in R, including all measured environmental variables and GPP can be found in the SI. Channel depth could not be including in the correlation plot, since there was less than one year of data available. (Fig. S2). In addition, we used stepwise regression to determine which environmental variables (out of salinity, air temperature, VPD, friction velocity (U*), PAR, or air pressure) were the strongest predictors of daily GPP during the growing season. We normalized the data by rescaling it between 0-1 for this regression to determine the size and direction of these effects. These results were supported by an AIC.

A random forest model trained on 2017-2018 data (i.e., normal salinity conditions) was used to predict daily GPP during 2014-2016 (i.e., drought-induced salinization period). Training variables included daily mean air temperature, channel depth, VPD, salinity, and U*, and total daily PAR. Random forests were run in R using the "caret" package.[53] Repeated cross validation was used for model assessment. The difference between the predicted and observed annual cumulative GPP in 2014-2016 represents the change in emissions caused by the salinization event.

Chapter 3: Results

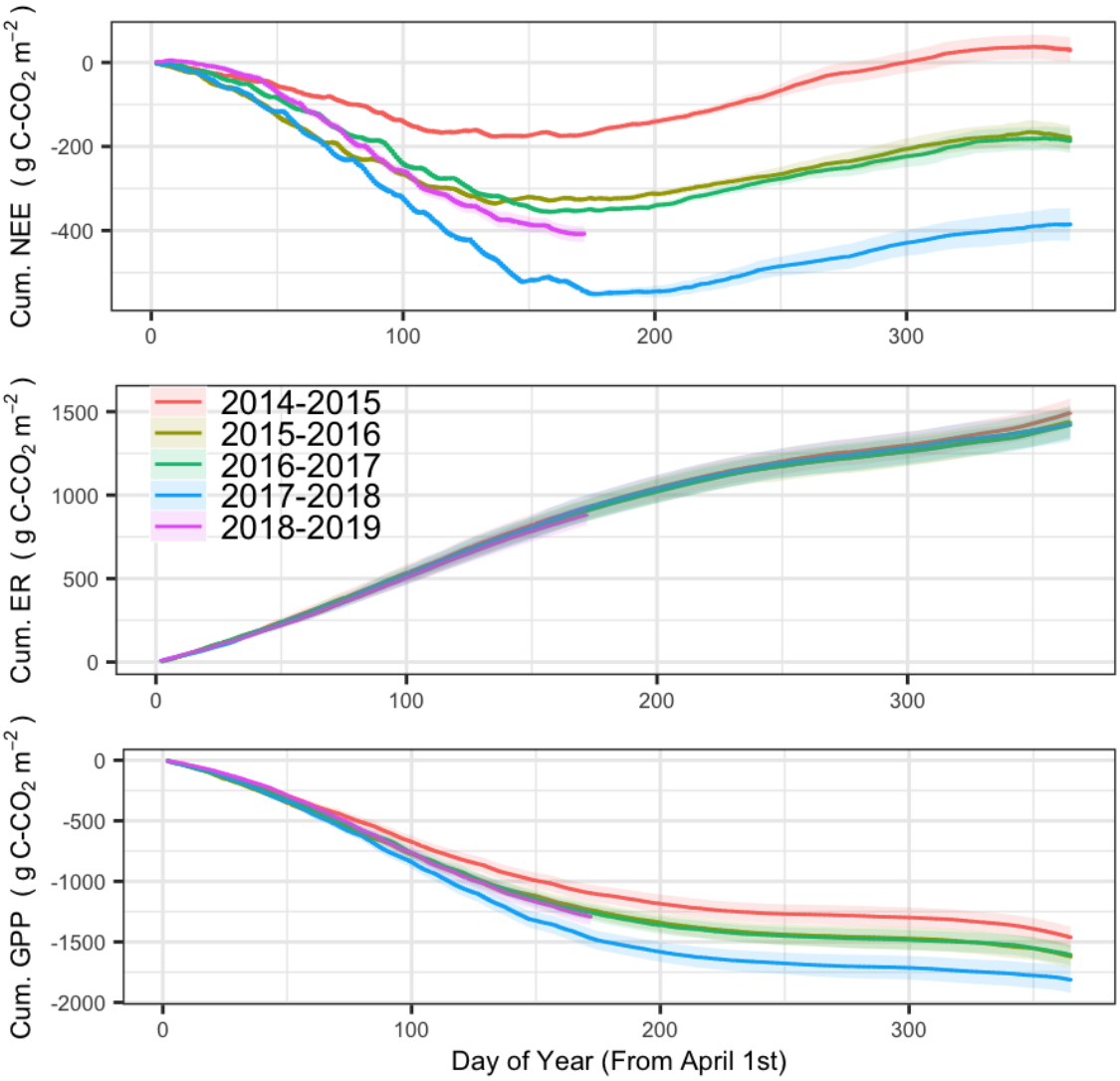

Figure 3. Cumulative net CO_2 Flux (NEE). NEE was partitioned using an artificial neural network trained on environmental variables that influence wetland GPP. Clouds around lines represent the 95% C.I. Ecosystem respiration (ER) was relative constant while gross primary productivity (GPP) differed between years.

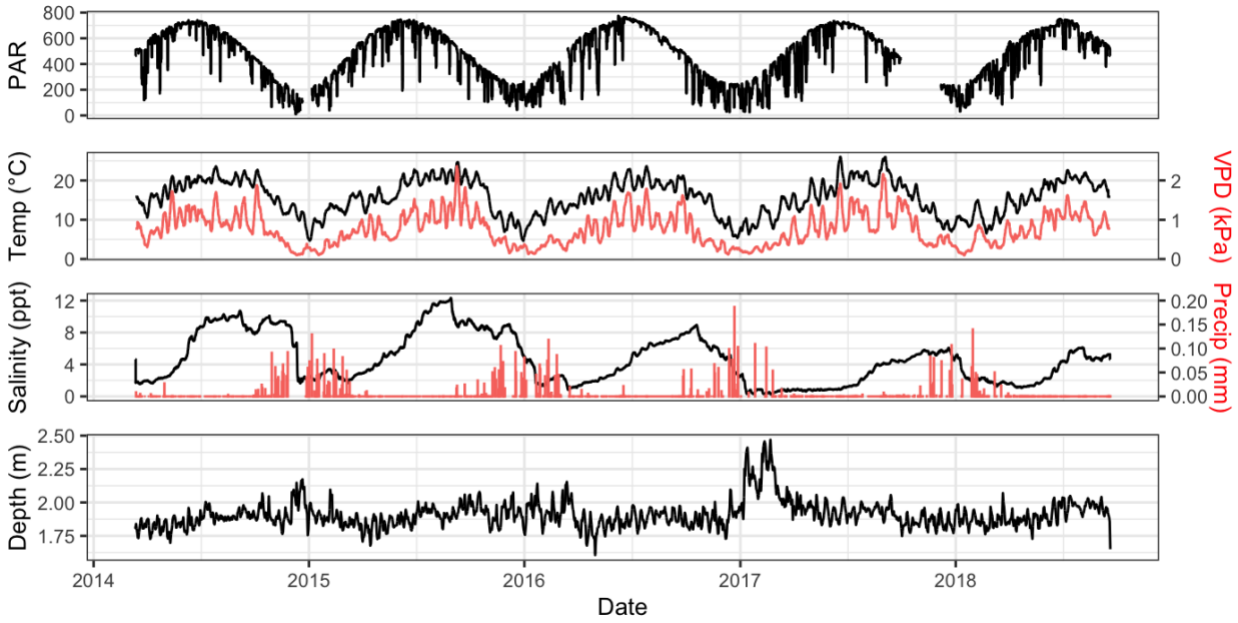

Figure 4. Environmental Data Timeseries. Salinization occurred at Rush Ranch from 2014 to early 2017, when heavy precipitation increased channel depth and salinity (daily rolling average ppt) returned to the baseline annual average of 4.5 ppt (2017-2018). PAR (daily rolling average µmol Photons m^{-2} s^{-1}), air temperature (weekly rolling average ºC), and VPD (weekly rolling average kPa) were more consistent between years. Red lines correspond to axes on the right.

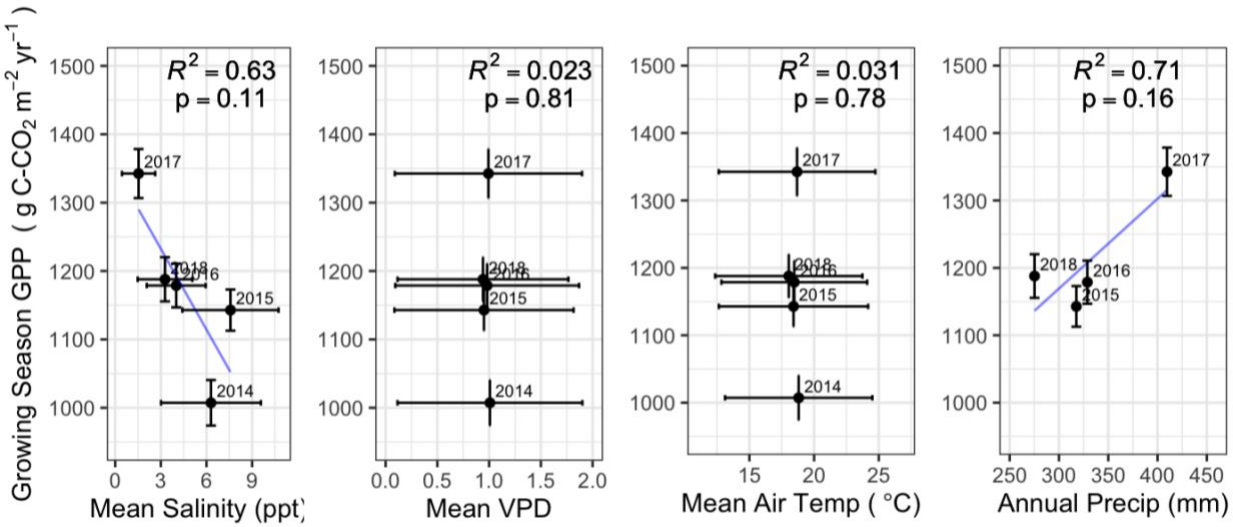

Figure 5. Response of Growing Season GPP to Environmental Drivers. Mean growing season (April-August) salinity, vapor pressure deficit, and air temperature were compared to total growing season GPP using linear regression. Total precipitation of the year prior (April-April) was compared to total growing season GPP. Horizontal bars indicate annual standard deviation of mean values. Vertical bars indicate 95% confidence interval of total GPP estimate, including gap-filling and ANN model error.

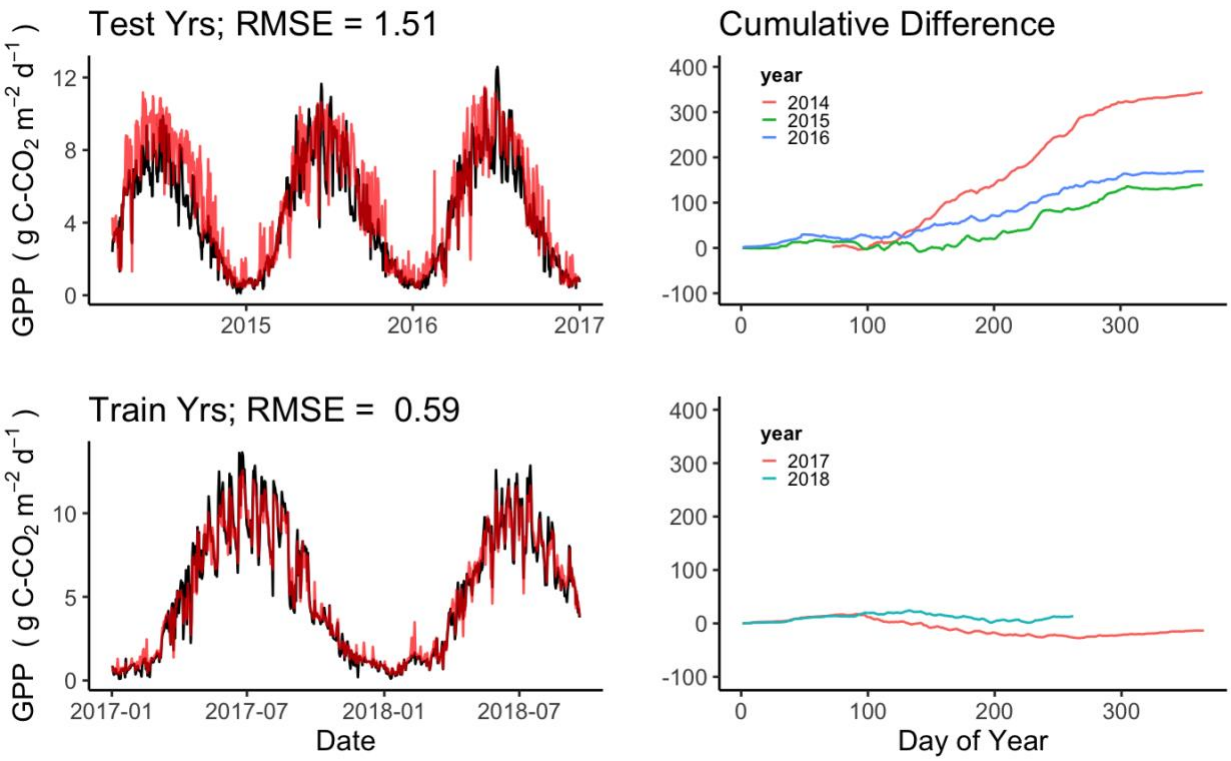

Figure 6. Observed (black) and modeled (red) gross primary productivity at Rush Ranch during 2014-2016. Modeled predictions were made using a random forest trained on 2017-2018 data, which were the years following the salinization event (bottom) and reflect baseline salinity conditions. The cumulative difference (Observed-Modeled) is shown for each year, in units of g $C\text{-}CO_2\ m^{-2}\ d^{-1}$. RMSE is shown as a measure of the increase in random forest error when modeling GPP during drought years.

Year	Observed GPP ($g\ C\ m^{-2}\ yr^{-1}$)	Predicted GPP ($g\ C\ m^{-2}\ yr^{-1}$)	GPP Reduction (%)
2014-2015	1468	1825	-24.3
2015-2016	1628	1779	-9.3
2016-2017	1472	1779	-9.8

Table 2. Annual GPP Reduction (%) Caused by the Salinization Event. This was estimated based on the difference between observed GPP and random forest model predicted GPP. Years were divided at April 1st, the beginning of the growing season.

Rush Ranch was a net sink of CO_2 for most of the drought years but showed significant year to year variability during this time (Fig. 2). The growing season of 2014, which marked the beginning of the drought period, was the only year where Rush Ranch was a net CO_2 source, releasing 29 (±15) g C m^{-2} in total from April 1st, 2014 to April 1st, 2015. During subsequent years, Rush Ranch was a net CO_2 sink, storing 181 (±14) and 187 (±14) g C m^{-2} in 2015-2016 and 2016-2017 respectively. The sink strength of Rush Ranch nearly doubled post-drought, storing 385 (±15) g C m^{-2} in 2017-2018.

Annual cumulative ER did not vary significantly across years, ranging from 1,423 (±42) g C m^{-2} in 2016-2017 to 1,496 (±43) C m^{-2} in 2014-2015 (Fig. 2; note the overlap of 95% C.I.). Annual cumulative GPP was lower during drought years (2014-2016) and recovered in 2017-2018. These trends were consistent between partitioning methods and were not a byproduct of

using an artificial neural network to partition fluxes (Fig S1). This suggests that annual variation in GPP was responsible for the variability of NEE at Rush Ranch during this period.

Out of all the measured environmental variables, mean annual salinity varied the most between years at the site (Fig. 3). During the drought years, average growing season salinity was 10.3 ppt, compared to the baseline growing season average of 4.5 ppt. Mean growing season salinity also had the strongest linear relationship with growing season GPP out of all tested environmental variables ($p = 0.11$, $R^2 = 0.63$; Fig 4).

Stepwise linear regression of daily data always included salinity in the best-performing models. Removal of salinity from these models resulted in a reduction in R^2 and increase in AIC score (Fig. S2). In all four best-performing models, salinity had a negative effect on GPP. Its standardized coefficient consistently had a magnitude of 0.2, meaning the size of salinity's effect on GPP was comparable to that of daily PAR (Table S1).

The random forest model, which was trained on post-drought data (i.e. naive to salinization), over-predicted GPP during the drought years of 2014-2016. Predicted GPP deviated from observed data at the beginning of each April and continued deviating throughout each growing season (Fig. 3, top). Late growing season GPP was especially over-predicted, coinciding with peak salinity during the year. According to the random forest model predictions, the salinization event caused a reduction in GPP of 25.9% in 2014-2015, 8.9% in 2015-2016, and 10.4% in 2016-2017 (Table 2). The year with the greatest reduction in GPP was not the year with the highest salinity, but the first drought year measured.

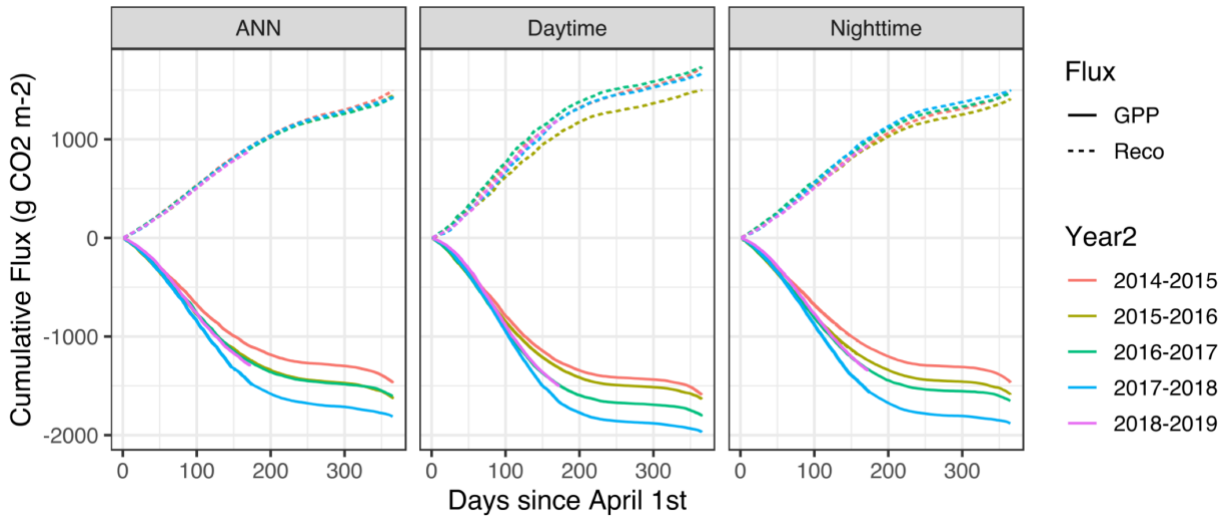

Figure 7. Cumulative gross primary productivity (solid) and ecosystem respiration (dotted) at Rush Ranch partitioned using the artificial neural network (ANN), daytime and nighttime approaches.

	Dependent var: GPP							
	(1)		(2)		(3)		(4)	
	+Sal	-Sal	+Sal	-Sal	+Sal	-Sal	+Sal	-Sal
(Int)	**-0.26*****	-0.31***	**-0.27*****	-0.31***	-0.25***	-0.31***	-0.1***	-0.15***
Air T	**0.8*****	0.64***	**0.72*****	0.62***	0.71***	0.62***	0.86***	0.71***
U*	**1.3*****	1.4***	**1.4*****	1.4***	1.3***	1.4***	1.3***	1.3***
PAR	**0.21*****	0.22***	**0.2*****	0.2***	0.21***	0.22***		
PA	**-0.032**	0.006			-0.032	0.006	0.001	0.043
VPD	**-0.1****	-0.028					-0.12**	-0.05
Salinity	**-0.2*****		**-0.2*****		-0.2***		-0.2***	
AIC	**6782**	6924	**6782**	6920	6784	6922	7103	7250
AIC df	**8**	7	**6**	5	7	6	7	6
R^2	**0.59**	0.55	**0.59**	0.55	0.59	0.55	0.57	0.53

Table 3. AIC comparing general linear models of daily GPP including (+Sal) and not including (-Sal) daily mean salinity as a driver. Variables were standardized (mean = 0, SD = 1) so that coefficient estimates represent drivers' relative effect size and direction. Drivers with negative coefficients reduce daily GPP. Significance codes: *=p<0.1; **=p<0.05; ***=p<0.01.

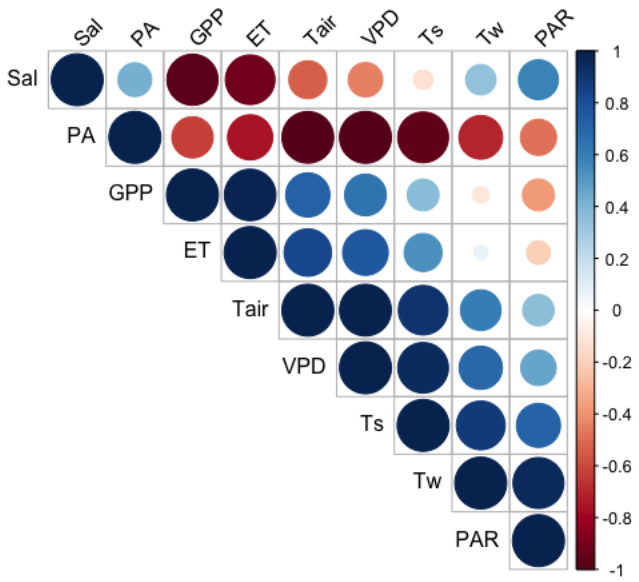

Figure 8. Correlation Plot of Growing Season (April – August) GPP Environmental Drivers, including mean salinity (Sal), air pressure (PA), evapotranspiration (ET), air temperature (Tair), vapor pressure deficit (VPD), soil temperature (Ts), and total growing season PAR. Positive correlation with GPP (blue circles) indicate drivers that promote photosynthesis. Environmental drivers are ordered by angular order of eigenvectors. This plot was made using the package 'corrplot' in R.

Chapter 4: Discussion

During a drought lasting from 2014 to 2017 in California, considerable variation in annual NEE was observed at our brackish tidal wetland site. Since ER was constant between years, this variation stemmed from variation in GPP (Fig. 2). Out of all environmental variables measured at this site, total growing season GPP showed the strongest negative correlation with mean salinity (Fig. 4; Fig. S2). This relationship was supported by stepwise linear regression of daily data (Table S1). We conclude that drought-induced salinization reduced GPP at this brackish tidal wetland, causing the observed reduction in NEE during drought years.

The threat of sea-level rise has drawn attention to the effect of increasing salinity on coastal ecosystems. Studies have linked increased salinity at coastal saltwater and freshwater wetlands to decreased plant productivity,[54,27] biomass,[55,56] and organic carbon mineralization,[57] but this relationship has not been as clear at brackish wetlands.[42] Some chamber studies have found that brackish wetland sediment respire more CO_2 than saline or freshwater wetlands[13,45] while others have found lower respiration at brackish wetlands.[58,59,42] Meanwhile, there have been few studies on the effect of salinity on brackish wetland biomass or plant productivity.

Experimental salinization of a plant free brackish peatland found that fluctuating salinity decreases NEE while constant elevated salinity has no effect.[60] The authors observed a reduction in surface water turbidity related to increased salinity and speculated that this could promote the growth of submerged macrophytes under higher salinity regimes.[60] This is unlikely in the present study as any change in surface water turbidity within the Rush Ranch tower footprint would have minimal effect on GPP, since it is a high marsh and is rarely submerged.[50]

In controlled lab studies, increasing soil salinity has long been known to decrease plant productivity. Within the first hours of salinization, plant cells reduce stomatal conductance to combat osmotic stress, suppressing leaf growth. Over longer periods of salinization, salt may enter the roots and shoots leading to ionic stress and eventually killing older leaves. Both mechanisms decrease productivity in plants lacking mechanisms of salt tolerance.[61]

Aquatic halophyte species have a range of salt tolerance.[62] As a brackish marsh, Rush Ranch is composed of a mixture of highly salt-tolerant species (i.e. *D. spicata*,[62] *L. latifolium*,[63] *S. pacifica*[64]) and a variably salt-tolerant genus (*Schoenoplectus* sp.[65]). However, salt tolerance does not guarantee stable productivity in response to fluctuations in salinity. *S. pacifica* is considered highly salt tolerant yet exhibits reduced growth under certain high salinity conditions.[64] Complicating the matter, aquatic halophytes can have intraspecific variation in salt tolerance depending on the salinity range to which an individual is acclimated.[62] Combined, these factors make it difficult to predict the range of salt tolerance of an entire brackish wetland ecosystem based only on its plant community.

Salinity and GPP are negatively related in saltwater coastal ecosystems that experience seasonal fluctuations in salinity. A mangrove forest in the Florida Everglades (15-30 ppt) exhibited a linear decrease in light use efficiency correlated with increasing salinity during its annual dry season.[66] A salt marsh on Plum Island, Massachusetts (26-40 ppt) has shown increased GPP during a period of high rainfall, which may have represented a desalinization event.[26] However, the authors found no relationship between salinity and GPP.[26]

At Rush Ranch, there was no correlation between growing season GPP and concurrent precipitation, but there was a non-significant positive correlation between growing season GPP and total precipitation from the preceding year (Fig. 3). This temporal delay in the effect of

rainfall highlights the importance of direct measurements of salinity in wetlands in the western United States, where wetlands are seasonally fed by melting snowpack and there is little to no rainfall during the growing season.

Mayberry wetland, a non-tidal freshwater wetland 20 km upstream of Rush Ranch along the San Joaquin River Delta, experienced a similar increase in salinity (~7 ppt) caused by the same drought and showed a 12% and 67% reduction in GPP during 2016 and 2017 respectively.[27] The reduction in GPP at Rush Ranch was 24% in 2014-2015, then 11% in 2015-2016, which is comparable to the initial response of the nearby Mayberry wetland.

Chapter 4: Conclusion

At Rush Ranch, we found that the 2011-2016 California drought caused a decrease in NEE that was driven by an underlying decrease in GPP. The key environmental driver of this decrease in GPP was salinity, which rose from a baseline average of 4.5 ppt to over 8 ppt during the growing season. This is one of the first studies to find a relationship between salinity and GPP at a brackish marsh.

Analyses in this study were limited by the available data. Atmospheric carbon fluxes were measured, but lateral carbon fluxes were not, meaning that net carbon uptake or loss at Rush Ranch could be different than the picture presented here. Air quality changes caused by wildfires throughout California, such as a possible increase in ozone, were not measured. Soil moisture, a key environmental driver of wetland carbon dynamics, was not measured at Rush Ranch until April 2016, mid-way through this study's timeline. Finally, flux and environmental data at Rush Ranch has been measured from 2014 to present. Inclusion of more years of data would increase confidence in the annual relationship between salinity and GPP observed in this study.

This study's conclusions would be further supported by additional performance review of its flux partitioning. This could be achieved by comparing nighttime NEE and ER partitioned by ANN, nighttime, and daytime methods.

Under climate change, extreme precipitation events such as droughts and flooding are expected to increase in frequency. We have shown that such events can cause variation in salinity that can suppress brackish tidal wetland GPP. This relationship should be included in models of coastal wetland carbon dynamics in order to accurately forecast multi-year carbon sequestration and support wetland restoration efforts.

References

1. Ipcc & IPCC. Climate Change 2013: The Physical Science Basis: Working Group I Contribution to the IPCC Fifth Assessment Report. *Annex 1* (2014) doi:10.1017/CBO9781107415324.Summary.
2. Le Quéré, C. *et al.* Global Carbon Budget 2018. *Earth Syst. Sci. Data* **10**, 2141–2194 (2018).
3. Baldocchi, D. 'Breathing' of the terrestrial biosphere: lessons learned from a global network of carbon dioxide flux measurement systems. *Aust. J. Bot.* **56**, 1 (2008).
4. Sweet, W. V. *et al.* Global and regional sea level rise scenarios for the United States. (2017) doi:10.7289/V5/TR-NOS-COOPS-083.
5. Thorne, K. *et al.* U.S. Pacific coastal wetland resilience and vulnerability to sea-level rise. *Sci. Adv.* **4**, eaao3270 (2018).
6. Hansen, L. T. The Viability of Creating Wetlands for the Sale of Carbon Offsets. *J. Agric. Resour. Econ.* 16 (2009).
7. Sapkota, Y. & White, J. R. Carbon offset market methodologies applicable for coastal wetland restoration and conservation in the United States: A review. *Sci. Total Environ.* **701**, 134497 (2020).
8. Murray, B. C., Pendleton, L., Jenkins, W. A. & Sifleet, S. Green payments for blue carbon: economic incentives for protecting threatened coastal habitats. *Green Paym. Blue Carbon Econ. Incent. Prot. Threat. Coast. Habitats* (2011).
9. Mcleod, E. *et al.* A blueprint for blue carbon: toward an improved understanding of the role of vegetated coastal habitats in sequestering CO $_2$. *Front. Ecol. Environ.* **9**, 552–560 (2011).

10. Tan, L. *et al.* Conversion of coastal wetlands, riparian wetlands and peatlands increases greenhouse gas emissions: A global meta-analysis. *Glob. Change Biol.* gcb.14933 (2019) doi:10.1111/gcb.14933.

11. Miller, R. L., Hastings, L. & Fujii, R. *Hydrologic Treatments Affect Gaseous Carbon Loss from Organic Soils, Twitchell Island, California, October 1995-December 1997*. (U.S. Department of the Interior, U.S. Geological Survey, 2000).

12. Oude Essink, G. & Kooi, H. Land subsidence and sea level rise threaten fresh water resources in the coastal groundwater system of the Rijnland water board, The Netherlands. in 227–248 (2012).

13. Poffenbarger, H. J., Needelman, B. A. & Megonigal, J. P. Salinity Influence on Methane Emissions from Tidal Marshes. *Wetlands* **31**, 831–842 (2011).

14. Bridgham, S. D., Cadillo-Quiroz, H., Keller, J. K. & Zhuang, Q. Methane emissions from wetlands: biogeochemical, microbial, and modeling perspectives from local to global scales. *Glob. Change Biol.* **19**, 1325–1346 (2013).

15. Goodrich, J. P., Varner, R. K., Frolking, S., Duncan, B. N. & Crill, P. M. High-frequency measurements of methane ebullition over a growing season at a temperate peatland site: PEATLAND CH $_4$ EBULLITION. *Geophys. Res. Lett.* **38**, n/a-n/a (2011).

16. Baldocchi, D. D. Assessing the eddy covariance technique for evaluating carbon dioxide exchange rates of ecosystems: past, present and future. *Glob. Change Biol.* **9**, 479–492 (2003).

17. Lasslop, G. *et al.* Separation of net ecosystem exchange into assimilation and respiration using a light response curve approach: critical issues and global evaluation: SEPARATION OF NEE INTO GPP AND RECO. *Glob. Change Biol.* **16**, 187–208 (2010).

18. Reichstein, M. *et al.* On the separation of net ecosystem exchange into assimilation and ecosystem respiration: review and improved algorithm. *Glob. Change Biol.* **11**, 1424–1439 (2005).

19. Oikawa, P. Y. *et al.* Revisiting the partitioning of net ecosystem exchange of CO2 into photosynthesis and respiration with simultaneous flux measurements of 13CO2 and CO2, soil respiration and a biophysical model, CANVEG. *Agric. For. Meteorol.* **234–235**, 149–163 (2017).

20. Maher, D. T., Call, M., Santos, I. R. & Sanders, C. J. Beyond burial: lateral exchange is a significant atmospheric carbon sink in mangrove forests. *Biol. Lett.* **14**, 20180200 (2018).

21. Megonigal, J. P. & Neubauer, S. C. Biogeochemistry of Tidal Freshwater Wetlands. in *Coastal Wetlands* 641–683 (Elsevier, 2009). doi:10.1016/B978-0-444-63893-9.00019-8.

22. Baldocchi, D. Measuring fluxes of trace gases and energy between ecosystems and the atmosphere - the state and future of the eddy covariance method. *Glob. Change Biol.* **20**, 3600–3609 (2014).

23. Schipper, L. A., Hobbs, J. K., Rutledge, S. & Arcus, V. L. Thermodynamic theory explains the temperature optima of soil microbial processes and high Q_{10} values at low temperatures. *Glob. Change Biol.* **20**, 3578–3586 (2014).

24. Brix, H. Gas exchange through dead culms of reed, Phragmites australis (Cav.) Trin. ex Steudel. *Aquat. Bot.* **35**, 81–98 (1989).

25. Kathilankal, J. C. *et al.* Tidal influences on carbon assimilation by a salt marsh. *Environ. Res. Lett.* **3**, 044010 (2008).

26. Forbrich, I., Giblin, A. E. & Hopkinson, C. S. Constraining Marsh Carbon Budgets Using Long-Term C Burial and Contemporary Atmospheric CO_2 Fluxes. *J. Geophys. Res. Biogeosciences* **123**, 867–878 (2018).

27. Chamberlain, S. D. *et al.* Effect of Drought-Induced Salinization on Wetland Methane Emissions, Gross Ecosystem Productivity, and Their Interactions. *Ecosystems* (2019) doi:10.1007/s10021-019-00430-5.

28. Laanbroek, H. J. Methane emission from natural wetlands: interplay between emergent macrophytes and soil microbial processes. A mini-review. *Ann. Bot.* **105**, 141–153 (2010).

29. Whalen, S. C. Biogeochemistry of Methane Exchange between Natural Wetlands and the Atmosphere. *Environ. Eng. Sci.* **22**, 73–94 (2005).

30. Byrd, K. B. *et al.* Forecasting tidal marsh elevation and habitat change through fusion of Earth observations and a process model. *Ecosphere* **7**, (2016).

31. Swanson, K. M. *et al.* Wetland Accretion Rate Model of Ecosystem Resilience (WARMER) and Its Application to Habitat Sustainability for Endangered Species in the San Francisco Estuary. *Estuaries Coasts* **37**, 476–492 (2014).

32. Li, T. *et al.* Field-scale simulation of methane emissions from coastal wetlands in China using an improved version of CH4MODwetland. *Sci. Total Environ.* **559**, 256–267 (2016).

33. Oikawa, P. Y. *et al.* Evaluation of a hierarchy of models reveals importance of substrate limitation for predicting carbon dioxide and methane exchange in restored wetlands: Model for Wetland Greenhouse Gas Fluxes. *J. Geophys. Res. Biogeosciences* **122**, 145–167 (2017).

34. State of California. Executive Order B-55-18 to Achieve Carbon Neutrality. https://www.ca.gov/archive/gov39/wp-content/uploads/2018/09/9.10.18-Executive-Order.pdf.

35. Hayward to consider revising emission reduction goals. https://www.hayward-ca.gov/discover/news/nov19/hayward-consider-revising-emission-reduction-goals.

36. United States Climate Alliance. Climate Leadership Across the Alliance. https://static1.squarespace.com/static/5a4cfbfe18b27d4da21c9361/t/5db99b0347f95045e051d262/1572444936157/USCA_2019+State+Factsheets_20191011_compressed.pdf.

37. Duarte, C. M., Middelburg, J. J. & Caraco, N. Major role of marine vegetation on the oceanic carbon cycle. 22 (2004).

38. BRIDGHAM, S. D. Carbon Dynamics and Ecosystem Processes. in *Ecology of Freshwater and Estuarine Wetlands* (eds. BATZER, D. P. & SHARITZ, R. R.) 185–202 (University of California Press, 2014).

39. Duarte, C. M., Dennison, W. C., Orth, R. J. W. & Carruthers, T. J. B. The Charisma of Coastal Ecosystems: Addressing the Imbalance. *Estuaries Coasts* **31**, 233–238 (2008).

40. Murray, N. J. *et al.* The global distribution and trajectory of tidal flats. *Nature* **565**, 222–225 (2019).

41. Pendleton, L. *et al.* Estimating Global "Blue Carbon" Emissions from Conversion and Degradation of Vegetated Coastal Ecosystems. *PLoS ONE* **7**, e43542 (2012).

42. Luo, M., Huang, J.-F., Zhu, W.-F. & Tong, C. Impacts of increasing salinity and inundation on rates and pathways of organic carbon mineralization in tidal wetlands: a review. *Hydrobiologia* **827**, 31–49 (2019).

43. Guo, H. & Pennings, S. C. Mechanisms mediating plant distributions across estuarine landscapes in a low-latitude tidal estuary. *Ecology* **93**, 90–100 (2012).

44. Bethke, C. M., Sanford, R. A., Kirk, M. F., Jin, Q. & Flynn, T. M. The thermodynamic ladder in geomicrobiology. *Am. J. Sci.* **311**, 183–210 (2011).

45. Chambers, L. G., Osborne, T. Z. & Reddy, K. R. Effect of salinity-altering pulsing events on soil organic carbon loss along an intertidal wetland gradient: a laboratory experiment. *Biogeochemistry* **115**, 363–383 (2013).

46. Michener, W. K., Blood, E. R., Bildstein, K. L., Brinson, M. M. & Gardner, L. R. Climate Change, Hurricanes and Tropical Storms, and Rising Sea Level in Coastal Wetlands. *Ecol. Appl.* **7**, 770–801 (1997).

47. Chambers, L. G., Reddy, K. R. & Osborne, T. Z. Short-Term Response of Carbon Cycling to Salinity Pulses in a Freshwater Wetland. *Soil Sci. Soc. Am. J.* **75**, 2000 (2011).

48. Capooci, M., Barba, J., Seyfferth, A. L. & Vargas, R. Experimental influence of storm-surge salinity on soil greenhouse gas emissions from a tidal salt marsh. *Sci. Total Environ.* **686**, 1164–1172 (2019).

49. Callaway, J. C., Borgnis, E. L., Turner, R. E. & Milan, C. S. Carbon Sequestration and Sediment Accretion in San Francisco Bay Tidal Wetlands. *Estuaries Coasts* **35**, 1163–1181 (2012).

50. Knox, S. H., Windham-Myers, L., Anderson, F., Sturtevant, C. & Bergamaschi, B. Direct and Indirect Effects of Tides on Ecosystem-Scale CO_2 Exchange in a Brackish Tidal Marsh in Northern California. *J. Geophys. Res. Biogeosciences* **123**, 787–806 (2018).

51. Knox, S. H. *et al.* Agricultural peatland restoration: effects of land-use change on greenhouse gas (CO_2 and CH_4) fluxes in the Sacramento-San Joaquin Delta. *Glob. Change Biol.* **21**, 750–765 (2015).

52. Wutzler, T. *et al.* Basic and extensible post-processing of eddy covariance flux data with REddyProc. *Biogeosciences* **15**, 5015–5030 (2018).

53. Kuhn, M. Building Predictive Models in *R* Using the **caret** Package. *J. Stat. Softw.* **28**, (2008).

54. Short, F. T., Kosten, S., Morgan, P. A., Malone, S. & Moore, G. E. Impacts of climate change on submerged and emergent wetland plants. *Aquat. Bot.* **135**, 3–17 (2016).

55. Sutter, L. A., Perry, J. E. & Chambers, R. M. Tidal Freshwater Marsh Plant Responses to Low Level Salinity Increases. *Wetlands* **34**, 167–175 (2014).

56. Zhou, M., Butterbach-Bahl, K., Vereecken, H. & Brüggemann, N. A meta-analysis of soil salinization effects on nitrogen pools, cycles and fluxes in coastal ecosystems. *Glob. Change Biol.* **23**, 1338–1352 (2017).

57. Baustian, M. M. *et al.* Relationships Between Salinity and Short-Term Soil Carbon Accumulation Rates from Marsh Types Across a Landscape in the Mississippi River Delta. *Wetlands* **37**, 313–324 (2017).

58. Nyman, J. A. & DeLaune, R. D. CO2emission and soil Eh responses to different hydrological conditions in fresh, brackish, and saline marsh soils. *Limnol. Oceanogr.* **36**, 1406–1414 (1991).

59. Wilson, B. J., Mortazavi, B. & Kiene, R. P. Spatial and temporal variability in carbon dioxide and methane exchange at three coastal marshes along a salinity gradient in a northern Gulf of Mexico estuary. *Biogeochemistry* **123**, 329–347 (2015).

60. van Dijk, G. *et al.* Salinization of coastal freshwater wetlands; effects of constant versus fluctuating salinity on sediment biogeochemistry. *Biogeochemistry* **126**, 71–84 (2015).

61. Munns, R. & Tester, M. Mechanisms of Salinity Tolerance. *Annu. Rev. Plant Biol.* **59**, 651–681 (2008).

62. Howard, R. J. & Rafferty, P. S. Clonal variation in response to salinity and flooding stress in four marsh macrophytes of the northern gulf of Mexico, USA. *Environ. Exp. Bot.* **56**, 301–313 (2006).

63. Picchioni, G. A., Hooks, T. N., Schutte, B. J., Shukla, M. K. & Daniel, D. L. Halophyte ion regulation traits support saline adaptation of Lepidium latifolium, L. draba, and L. alyssoides. *Plant Ecol.* **221**, 295–308 (2020).

64. Schile, L. M., Callaway, J. C., Parker, V. T. & Vasey, M. C. Salinity and Inundation Influence Productivity of the Halophytic Plant Sarcocornia pacifica. *Wetlands* **31**, 1165–1174 (2011).

65. Watson, E. B. & Byrne, R. Recent (1975–2004) Vegetation Change in the San Francisco Estuary, California, Tidal Marshes. *J. Coast. Res.* **28**, 51 (2012).

66. Barr, J. G. *et al.* Controls on mangrove forest-atmosphere carbon dioxide exchanges in western Everglades National Park: MANGROVE CARBON DIOXIDE EXCHANGE. *J. Geophys. Res. Biogeosciences* **115**, n/a-n/a (2010).